On the Stability of RSRP and Variability of Other KPIs in LTE Downlink – An Open Dataset

Vaclav Raida
Technische Universität Wien
Vienna, Austria
vaclav.raida@tuwien.ac.at

Philipp Svoboda
Technische Universität Wien
Vienna, Austria
philipp.svoboda@tuwien.ac.at

Martin Koglbauer
A1 Telekom Austria
Vienna, Austria
martin.koglbauer@a1.at

Markus Rupp
Technische Universität Wien
Vienna, Austria
markus.rupp@tuwien.ac.at

***Abstract*—In this paper, we discuss the temporal behavior of several key parameter indicators (KPIs) in LTE downlink (DL) based on multiple long-term static measurement campaigns conducted under various conditions, including rural and urban indoor and outdoor scenarios. We publish part of the measurements as an open dataset. We conclude that the reference signal received power (RSRP) does not show any time-of-day patterns and thus can be modeled as time-invariant for limited periods of time (from several hours to multiple days) followed by occasional anomalies in the form of jumps of several dB. The other KPIs, for example, throughput, exhibit repeated diurnal patterns with significant differences between peak hours (full cell in the afternoon and evening) and off-peak hours (empty cell in the early morning). Even under model idealizations, such KPIs should be thus modeled at least as cyclostationary random processes. We are not aware of any other paper that would provide static LTE DL measurement data covering several weeks and would thus allow the scientific community to study the diurnal patterns without a need to perform own measurements.**

***Index Terms*—dataset, cellular, mobile, network, LTE, measurement, static, RSRP, RSRQ, throughput, indoor, outdoor, rural, urban, crowdsourcing, 5G**

I. Introduction

For realistic network modeling and simulations, reliable baseline measurements are necessary. In cellular mobile networks, many key parameter indicators (KPIs) perceived by a user under test are subject to the, throughout the day varying, activity of other users. To capture such diurnal patterns, sufficiently long static measurements are necessary.

Measurement results in a single, static location vary significantly based on the time of day. Measurements under mobility scenarios allow investigating spatial properties and the impact of users' speed but cannot reveal the quality of service differences between the peak hours and off-peak hours. The current research papers either provide no open datasets or offer only measurements, the duration of which is limited to tens of minutes (see Section I-B).

In this paper, we provide an open dataset [1] that contains reference signal received power (RSRP) [2], reference signal received quality (RSRQ) [2], and application layer throughput R, measured in LTE downlink (DL) in live, operational networks in three static locations. RSRP measures signal strength, RSRQ depends on the cell load (see Section I-B), DL throughput captures the quality of service experienced by end-users. These are the three KPIs that are reported by most of the commercial LTE devices [3].

Additionally, we evaluate repeated static crowdsourced measurements of RSRP and RSRQ provided by an Austrian operator. As we have performed our controlled measurements with of-the-shelf user equipment (UE), dataset [1] well represents characteristics of crowdsourced scenarios, e.g., [4]. Finally, we summarize the temporal behavior of the individual KPIs.

Our measurements span several weeks, during which we sampled the KPIs regularly. The shape of a time-of-day trend depends on the behavior of the population served by a specific cell (e.g., university campus, administrative buildings, tourist area). Our dataset can help other researchers to decide how long to measure to estimate the shape of the trend. As the diurnal patterns are correlated in time, the dataset can also help to optimize the sampling strategy and reduce the number of required samples.

A. Paper Outline

Section II presents the most extended scenario that comprises 56 days of static outdoor measurements in a rural area conducted with a rooted smartphone. Particular measurement intervals were impacted by rain (included in the dataset).

Section III provides details about two outdoor locations in a dense urban environment. Both measurements were one week long, and we conducted them with LTE modems.

Section IV analyzes crowdsourced measurements of RSRP and RSRQ, which were collected by a mobile network operator (MNO) from users' static indoor LTE modems (not a part of the dataset due to our nondisclosure agreement with the MNO). In our analysis, we processed time-series of 1074 users. Each time-series was seven days long.

In Section V we conclude the paper. Whereas RSRP can be modeled as time-invariant for multiple days with the standard deviation below $0.5\,\mathrm{dB}$, RSRQ and DL throughput reveal periodic, time-of-day dependent variations. We expect similar KPI behavior in 5G frequency range 1.

B. Related Work

Multiple papers [6]–[9] discuss time-of-day effects in LTE KPIs. Unfortunately, none of them offers the measurements as open data or at least a mathematical model to enable other researchers to study the time-of-day effects in more detail.

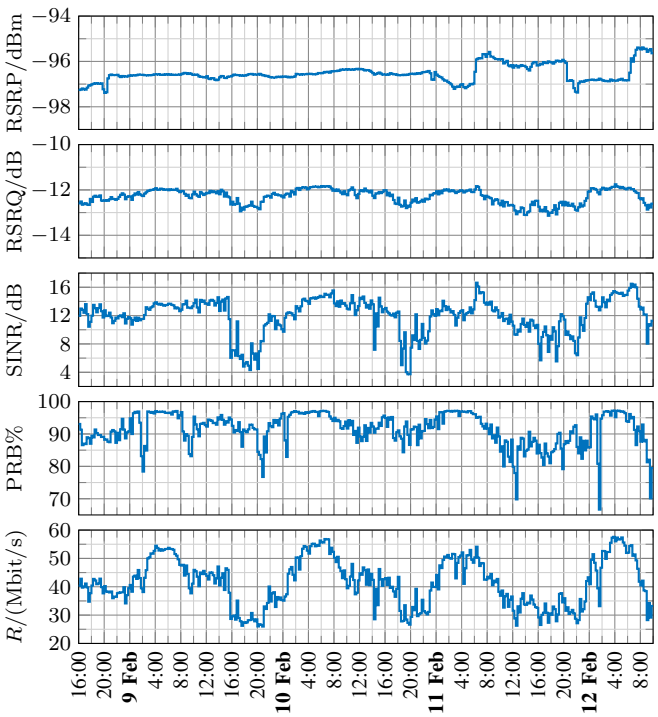

Fig. 1. Ninety hours of static urban indoor LTE DL measurements collected by Keysight's NEMO phone. In this visualization, the original samples with the granularity of 0.5 s are binned to 15 min intervals. We presented detailed results in our previous paper [5].

Kumar et al. [6] measured four locations on the university campus over one week with a passive LTE sniffer (open implementation on a software-defined radio) and observed diurnal patterns in the number of active users and resource block utilization. Polaganga and Liang [9] processed eNodeB logs provided by an MNO and confirmed strong diurnal patterns in the number of active users and DL throughput.

Cainey et al. [7], who analyzed crowdsourced LTE DL measurements from Opensignal, and Sommers and Barford [8], who evaluated crowdsourced cellular measurements from Ookla's Speedtest, both detected time-of-day dependencies with significant differences between peak and off-peak hours.

The current LTE open datasets [10]–[14] (see [5] for details) are either too short (less than one hour) or stem from mobile campaigns and thus do not allow to examine diurnal patterns, which span several hours, in static locations.

In [5], [15], we have provided 90 hours of static LTE DL measurements (Fig. 1) conducted with Keysight's NEMO UE [16] in an urban indoor environment. We collected a dataset [15] with a specialized measurement UE; therefore, it contains more KPIs with higher resolution. In this paper, we add three outdoor campaigns performed with commercial UEs, which better represent measurements obtainable by off-the-shelf devices and from crowdsourcing databases such as [4]. Dataset [1] also covers a longer time interval than that in [15].

In general, RSRQ depends on RSRP, cell load, and noise and interference power P_Z [17]. For a specific range of RSRP and P_Z, RSRQ becomes independent of RSRP and P_Z and is only a function of the cell load, see [17, Fig. 2]. We conducted the measurements [5], [15] during an uninterrupted download of as much data as possible. The cell load of the serving eNodeB was thus close to 100% all the time. Therefore, the RSRQ in Fig. 1 is relatively stable, with the standard deviation of ca. 0.32 dB.

In the dataset [1], which we provide here, we measured the DL throughput by triggering a short iPerf 3 [18] test from time to time. RSRQ samples presented in the following sections thus reflect the cell load caused by other users and show higher variability than RSRQ in Fig. 1.

II. Rural Outdoor Smartphone-Measurement

In this section, we present details about measurements that we were conducting in an operational LTE network (band 20, LTE 800) of an Austrian MNO in a rural area near Kindberg (latitude 47.5093, longitude 15.4569), Austria, between 8 September and 3 November 2016.

A. Hardware Setup and Measurement Procedure

The measuring UE was a rooted LG K4 [19] smartphone, LTE Cat. 4 [20]. The UE was locked in a shielding box (rain protection) with two external antennas (2×2 MIMO).

We coded a custom Android Java application for repeatedly triggering an iPerf 3 DL throughput measurement every ca. 60 minutes and for passively collecting the signal values and cell information from Android Telephony API [3], [21].

We used our own iPerf 3 server located at the Institute of Telecommunications, TU Wien. Five parallel TCP connections and the CUBIC congestion control algorithm (default in most of the smartphones) provided a sufficiently fast throughput ramp-up. We set the measurement duration to 10 s.

The Android API was updating the reported values every two seconds. To not miss any samples, our application was sampling from the API ca. once per second. The amplitude resolution was 1 dB for RSRP and 0.5 dB for RSRQ.

B. Dataset Structure

The table `signal_samples.csv` contains four columns: Unix timestamp, RSRP, RSRQ, and cell ID. As the Android API provides signal values not only for the serving cell but also for the neighboring cells, there are multiple samples for a single timestamp. In total, three distinct cells were detected. For PCI[1] A, there are 4.2 million samples. PCI B has 4.1 million samples, and PCI C only 1605.

The table `serving_cell.csv` identifies the serving cell for each timestamp. PCI A was the serving cell in 4.0 million cases and PCI B in 220 thousand cases. PCI C was never serving the measurement UE. There are 75 timestamps that correspond to PSC (primary scrambling code) D; in these rare cases, the UE switched from LTE to UMTS. The throughput values estimated by iPerf 3 are in the table `iperf.csv`. The timestamp always corresponds to the test start.

Fig. 2 displays three-hour averages of measured RSRP and RSRQ for PCI A and B, and of the DL application layer throughput R. Until 23 October, where the RSRP of PCI B prevails, PCI A was almost exclusively the serving cell.

[1]Physical cell ID. We anonymized cell identities in our dataset.

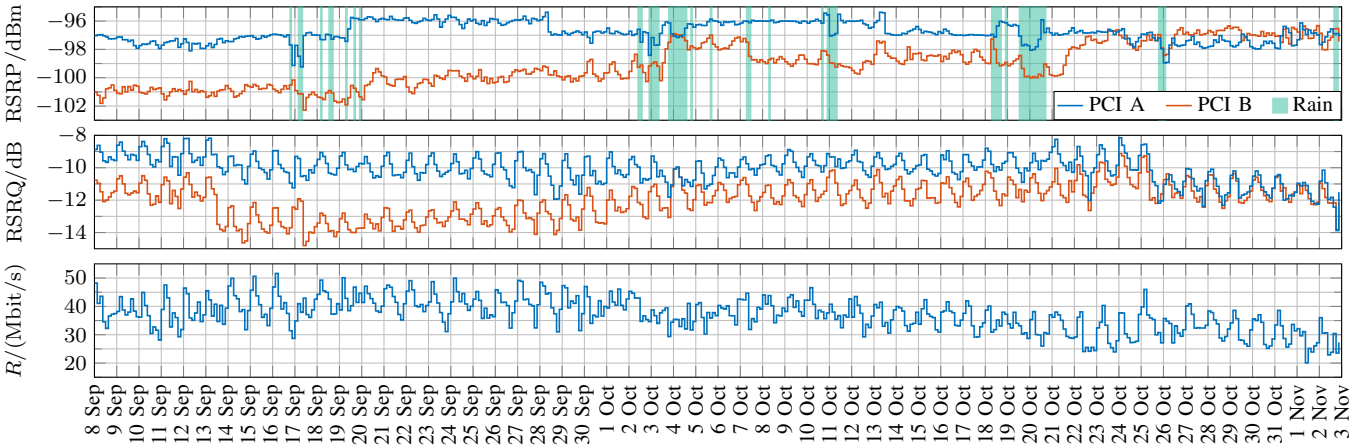

Fig. 2. Fifty-six days of static outdoor LTE DL measurements in a rural area in an operational network of an Austrian MNO. The measuring UE detected two cells, PCI A and PCI B. Until 23 October, the UE was served mainly by PCI A; then mainly by PCI B. RSRP of the serving cell features long time-invariant intervals interrupted by occasional jumps. Some of the short-term anomalies can be explained by rain. Measurements of the RSRP of the non-serving cell are less stable than those of the serving cell. RSRQ and throughput show strong time-of-day dependency.

C. Observations: KPI Behavior

RSRQ and throughput show almost periodic behavior with minima during peak hours (full cell in the afternoon and evening) and maxima in the off-peak hours (empty cell in the early morning). In the RSRP trace of the serving cell, we can observe long stable intervals independent of the time of day. For example, the standard deviation of serving RSRP is $0.20\,\mathrm{dB}$ between 19 and 28 September (ca. 10 days) and $0.13\,\mathrm{dB}$ between 4 and 10 October (ca. 7 days). In the same intervals, the standard deviation of the RSRQ is $0.58\,\mathrm{dB}$ (2.9 times higher than for RSRP) and $0.59\,\mathrm{dB}$ (4.5 times higher than for RSRP) and throughput ranges from 30 to $50\,\mathrm{Mbit/s}$.

Between the long stable RSRP intervals, we see occasional jumps of $\approx 1\,\mathrm{dB}$. As we measured in an operational network, it is merely impossible to identify the root of the jumps. It might be a change in eNodeB's transmit power. Or, it might be a nearby parked metal van that shadows electromagnetic waves incoming from a particular direction and causes a different multipath component to become dominant.

Apart from stable intervals and occasional jumps, the RSRP also exhibits several short-term anomalies. Some of the RSRP deviations can be explained by rain. Wet surfaces and wet external antennas significantly impact the wave propagation. Precipitation data from a nearby weather station are included in the table `rain.csv`. Time-resolution is 10-minutes. Each timestamp identifies the end of a ten-minute interval, during which the rainfall (in millimeters) was measured.

The neighboring cell exhibits higher RSRP variability than the serving cell. Since the neighboring cell has on average a lower RSRP compared to the serving cell, a possible explanation could be that the RSRP stability decreases with decreasing signal power. However, in Section IV we will see that the negative correlation between the RSRP standard deviation and the RSRP mean is very low. We thus suspect that an increased variance is not caused by the absolute signal power, but by the presence of a stronger cell (the serving cell), which reduces the accuracy of the measured neighboring RSRP.

III. Dense-Urban Outdoor Modem-Measurements

In this section, we describe two outdoor measurements performed at the Institute of Telecommunications, TU Wien, located in the city center of Vienna. The first measurement took place on the institute's rooftop (line-of-sight) from 22:00 on 10 October to 22:00 on 17 October 2019. The second measurement was conducted in the institute's inner courtyard (non-line-of-sight) from 8:00 on 28 October to 8:00 on 4 November 2019. We performed both measurements in an operational LTE network (band 7, LTE 2600) of an Austrian operator.

A. Hardware, Measurement Procedure, and Dataset Structure

In both measurements, we used LTE modem Huawei E5180 [22], LTE Cat. 4 [20], connected to a Raspberry Pi 3 B [23]. A cron job on the Raspberry Pi was triggering an iPerf 3 DL measurement (10 parallel TCP connections, 60 minute test duration, Reno congestion control algorithm) every 15 minutes. We used the same iPerf 3 server as in Section II. For each measurement, the table `iperf.csv` contains a timestamp of the test start and the measured DL throughput.

We configured a band lock on the modem to prevent handovers. Unlike the smartphone in Section II, the modem does not provide access to signal values of the neighboring detected cells. Therefore, the table `signal_samples.csv` contains only Unix timestamps, RSRP, and RSRQ, but no cell ID—all samples in the table correspond to a single eNodeB. Note, however, that the cell in the rooftop-scenario was a different one than in the courtyard-scenario. The RSRP and RSRQ values are logged as 15-minute linear averages. The timestamp corresponds to the beginning of the 15-minute bin.

B. KPI Behavior

Let us first discuss the rooftop-scenario in Fig. 3 (a). The mode (the most frequent value) of RSRP equals $-75.5\,\mathrm{dBm}$ and matches approximately the 10-percentile (the distribution is thus quite skew). Apart from many positive (by ca. $+0.5\,\mathrm{dB}$) short-term deviations from the mode, we observe a strong anomaly between 8:00 and 12:00 on 16 October.

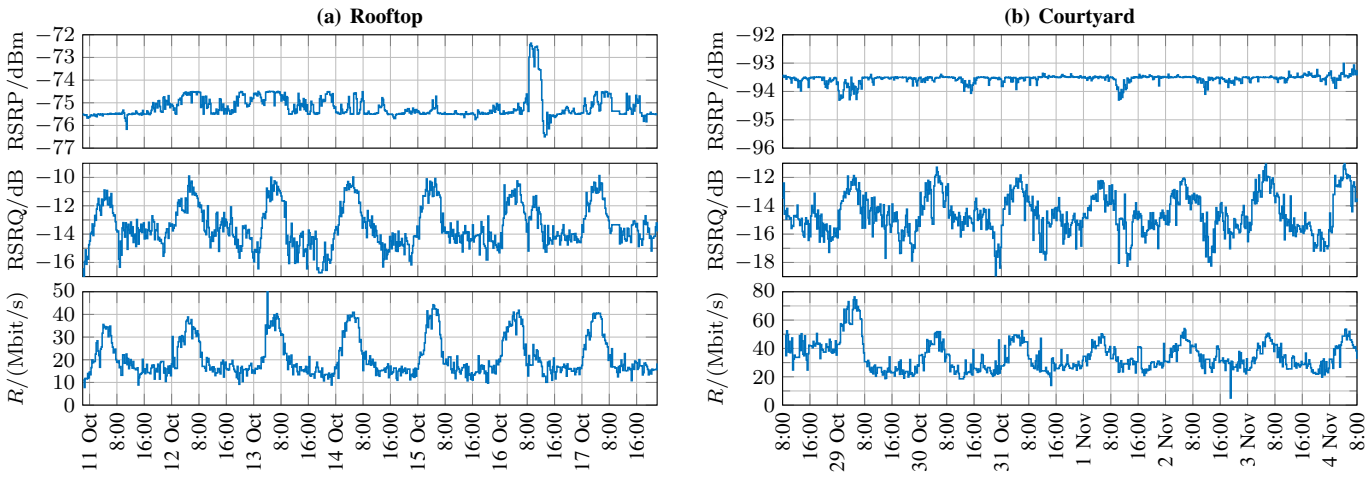

Fig. 3. One week of LTE DL measurements conducted with an LTE modem and Raspberry Pi in an operational network of an Austrian MNO in a dense urban environment. (a) Measurements were conducted on the rooftop of the Institute of Telecommunications, TU Wien. (b) Measurements were collected at the institute's inner courtyard.

Nevertheless, RSRP shows no periodic patterns and is quite stable—the standard deviation is $0.50\,\mathrm{dB}$ if we consider all samples, and $0.35\,\mathrm{dB}$ if we exclude the anomaly on 16 October. On the contrary, throughput R regularly ranges from 10 to $40\,\mathrm{Mbit/s}$ with periodic time-of-day dependency. RSRQ is highly correlated with R (correlation coefficient $\rho = 0.85$) and ranges from -16 to $-10\,\mathrm{dB}$. The RSRQ standard deviation is about three times higher ($1.52\,\mathrm{dB}$) compared to RSRP.

In the courtyard-scenario, Fig. 3 (b), the KPI behavior is similar. RSRP is even more stable than in (a), with the standard deviation of $0.15\,\mathrm{dB}$ and only a few irregular notches of up to $-0.8\,\mathrm{dB}$. RSRP again shows no periodic daytime dependency. The RSRP distribution has opposite skewness than in (a)—the mode of $-93.5\,\mathrm{dBm}$ corresponds to ca. 90-percentile.

Most of the RSRQ values range from -11 and $-18\,\mathrm{dB}$; the standard deviation ($1.46\,\mathrm{dB}$) is almost ten times higher compared to RSRP. The correlation coefficient between RSRQ and throughput is lower, only 0.62, due to a throughput irregularity: During the first 24 hours, the throughput is significantly higher (25 to $75\,\mathrm{Mbit/s}$) than in the rest of the week (mostly 20 to $50\,\mathrm{Mbit/s}$), which may be caused by a lower interference from neighboring cells. If we consider only samples from 30 October on, the correlation coefficient increases to 0.73.

IV. Crowdsourced Urban Indoor Measurements Collected from End-Users' LTE Modems

In this section, we present crowdsourced measurements provided by an Austrian MNO. The MNO collected anonymized data with a network monitoring tool from end-users' LTE modems. The data contain a single modem-type, LTE Cat. 4, in the 4th district of Vienna. Due to our nondisclosure agreement with the MNO, we are not allowed to share this section's data. They are thus not included in our open dataset [1].

A. Measurement Structure and Preprocessing

The data cover one week, from 25 January to 1 February 2019. Time-series have a 15-minute resolution. For each 15-minute bin, we obtain RSRP and RSRQ linear averages, cell IDs, and the number of handover attempts/successes/failures. As we cannot force the users to actively download data, throughput measurements are not available.

A random ID identifies each modem. We know that all modems are located in the 4th district. However, we do not know the exact modem location nor identity of the customers. Measurements are appropriately anonymized. Nevertheless, we assume that most of the modems are static and indoor.

For a single user, multiple cells are often reported. The strongest cell (the highest RSRP) has more samples than the weaker cells. However, even for the most frequently reported cells, some 15-minute bins are occasionally missing. For each user, we identify the most frequently reported cell and select only those 15-minute intervals, which contain no handovers.

Since calculating any statistics from a small number of samples is always doubtful, we excluded users that provided less than 100 samples for their most frequently reported cell. We ended up with time-series from 1074 unique users.

B. Diurnal Patterns of RSRQ and Jumps of RSRP

To better understand the behavior of the RSRP and RSRQ in noncontrolled crowdsourced measurements, we have calculated the standard deviation of RSRP for each user and examined the time-series of the extreme cases. Fig. 4 (a) presents three users (1a–3a) from the set with the lowest RSRP standard deviation. Fig. 4 (b) shows three users (1b–3b) from the set with the highest RSRP standard deviation. We picked the users 1a–3a and 1b–3b from larger groups of users with similar standard deviations such that user 1a has a similar RSRP average as user 1b, user 2a has a similar average as user 2b, and user 3a has a similar average as user 3b.

RSRQ exhibits diurnal patterns in both (a) and (b). In (a), RSRP is almost time-invariant. Although in (b), RSRP has a higher standard deviations than the corresponding RSRQ, the behavior of RSRP is qualitatively different. The high standard deviation of RSRP is not caused by periodic time-of-day effects but by occasional jumps of several dB, after which RSRP remains stable for hours or even days.

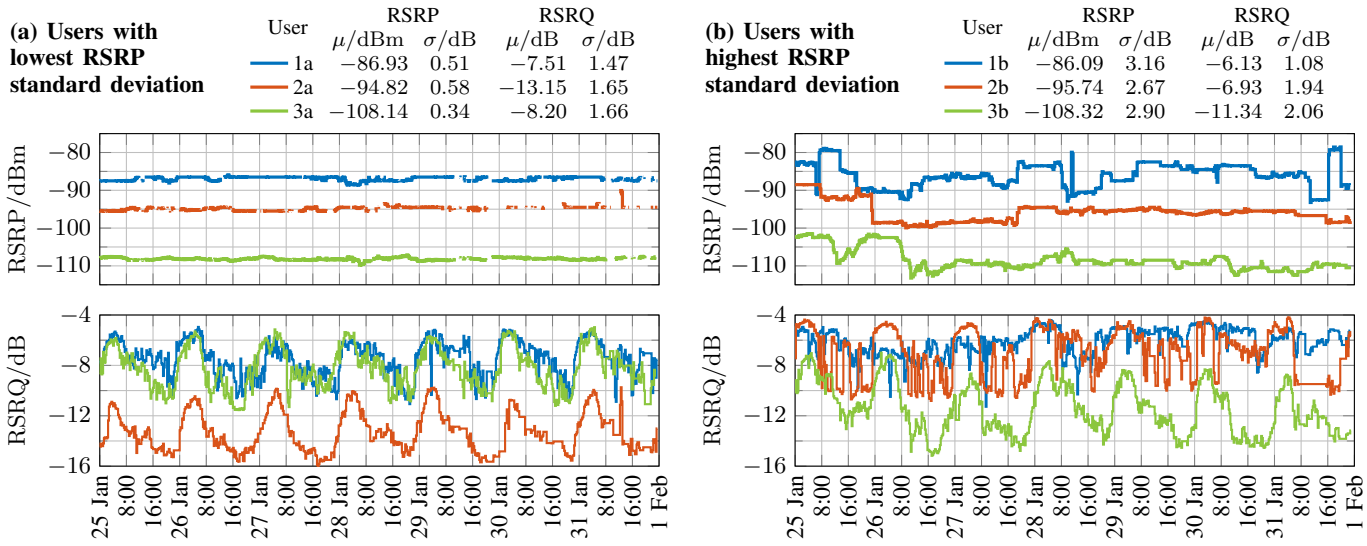

Fig. 4. An example of users' RSRP and RSRQ time-series. From in total 1074 users, we chose three users (1a, 2a, 3a) from ten users with the most stable RSRP (lowest RSRP variance) in (a), and three users (1b, 2b, 3b) from ten users with the least stable RSRP (highest variance) in (b), such that the displayed RSRP traces have similar RSRP means (1a vs. 1b, 2a vs. 2b, 3a vs. 3b) regardless of the RSRP variance. We can thus conclude that the qualitatively different behavior of RSRP in (a) and (b) is not caused by lower/higher RSRP mean but instead by environmental influences (e.g., changes in user's apartment).

Even with a UE in a controlled static room with no human activity in [5], RSRP jumps may occur (Fig. 1), since we have no control over the environment between the UE and the eNodeB. In a crowdsourced scenario, RSRP jumps can have additional causes, such as a shift of the measuring modem, moved furniture, metal window blinds pulled up/down.

From [17, Fig. 2 and 4], we know that for a specific range of RSRP, the RSRQ values are independent of RSRP. It is thus no surprise that the order of RSRQ traces in (a) does not match the order of RSRQ traces in (b), although the RSRP averages 1a-3a are very similar to 1b–3b.

Fig. 5 depicts the empirical CDFs of RSRP standard deviations (blue solid) and RSRQ standard deviations (red dash-dotted) based on 1074 UEs. For each UE, the standard deviation is calculated from the whole time-series (one week).

C. Twenty-Four-Hour Window

Comparing RSRP variance with RSRQ variance based on the whole week in Fig. 5 may be misleading. RSRQ regularly alternates, reaching a minimum during peak hours and a maximum in the off-peak hours. RSRP in Fig. 4 (b) reaches a higher standard deviation than RSRQ, but only due to a few occasional big jumps (up to 12 dB) in an otherwise flat curve. Except for these "anomalies," RSRP may remain stable for several days (e.g., user 2b between 28 and 31 January).

To reduce the impact of RSRP anomalies, we calculate the standard deviation for each position of a 24-hour sliding window. For each user, we select the minimum RSRP standard deviation and minimum RSRQ standard deviation among all window positions.[2] Any window position always contains all 24 day-hours and thus reflects the variability due to diurnal patterns. At the same time, if the quantity of interest suffers from anomalies, which are not too frequent, there is a higher chance (compared to the calculation based on the whole week) that at least one window position contains no anomalies.

[2]The selected window for RSRP may be different than the selected window for RSRQ. We thus do not favor any of the two quantities.

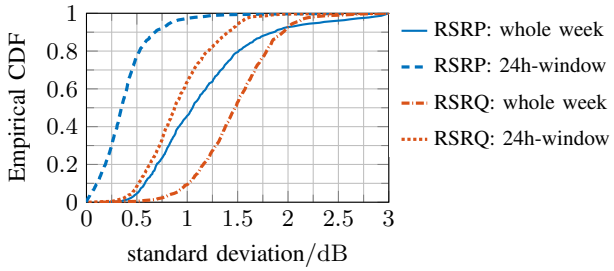

Fig. 5. Distribution of RSRP and RSRQ standard deviation based on time-series of 1074 users. In the first case, we calculated the standard deviation of each user based on the whole week. In the second case, we considered only the standard deviation in each user's most stable 24-hour window.

If we now compare the distribution of RSRP standard deviations (blue dashed) and RSRQ standard deviations (red dotted) calculated from the most stable 24-hour windows, we see that the distance between them increased dramatically. The difference between 90-percentiles of RSRP and RSRQ standard deviations was only 0.08 dB when considering the whole week. The windowed approach leads to a 90-percentile of RSRP standard deviation (0.69 dB) that is only half of the 90-percentile of RSRQ standard deviation (1.41 dB).

D. RSRP Distribution

For 97% of users, the standard deviation of RSRP in the most stable 24-hour window was below 1 dB (Fig. 5). Fig. 6 (a) shows the scatter plot with users' RSRP mean and standard deviation in the most stable window. We were interested in whether the RSRP values fluctuate more at lower signal strength. However, we found only a weak negative correlation between the standard deviation and mean. The correlation coefficient is $\rho = -0.15$.

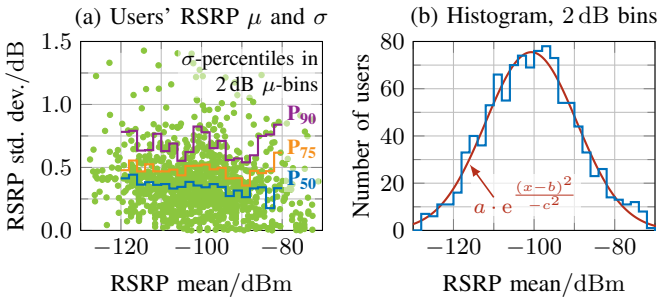

Fig. 6. (a) Scatter plot visualizing RSRP of 1074 users. Each dot represents one user and his/her RSRP mean μ and RSRP standard deviation σ within the most stable 24-hour window (window with the lowest RSRP σ). RSRP μ and σ are only weakly correlated with the correlation coefficient $\rho = -0.15$. Color lines show 50, 75, and 90-percentiles of σ for each 2 dB wide μ-bin. (b) Histogram of users' RSRP means μ and fitted scaled normal distribution $a \cdot \exp\left(-(x-b)^2/c^2\right)$ with $a = 75.47$, $b = -100.70$, and $c = 16.03$.

To visualize the density of the points in Fig. 6 (a), we binned RSRP mean (2 dB step size) and plotted percentiles (90, 75, and 50) of the standard deviation for each bin. Fig. 6 (b) shows the corresponding number of samples in each RSRP-mean bin. A linear least-squares fit $a \cdot x + b$ to the 50-percentile values P_{50} in (a) results in coefficients $a = -3.38 \cdot 10^{-3}$ and $b = 4.6 \cdot 10^{-3}$. The slope a corresponds to an approximately -0.14 dB decrease in RSRP standard deviation when RSRP mean increases by 40 dB.

V. Conclusion

As we have seen not only in our controlled campaigns but also in the crowdsourced measurements, RSRQ and downlink throughput R exhibit clear diurnal patterns, reaching minima in peak hours (full cells in the afternoon and evening) and maxima in off-peak hours (empty cells in the early morning). In an idealized case, RSRQ and R can be modeled as cyclostationary random processes.

On the other hand, RSRP remains stable for longer periods of time—from several hours to many days—with occasional jumps. Thus, in the simplest case, RSRP can be modeled as a time-invariant quantity. A more realistic model should contain an occurrence of anomalies, which may change the RSRP mean by several dB.

We had no prior knowledge of long-term KPI behavior. We thus measured for several weeks and sampled the KPIs regularly. Although the shape of the diurnal patterns may differ based on a specific user population, we hope that our dataset helps other researchers to optimize their sampling process and measurement duration. For example, for RSRP, only a change detection may be employed. For RSRQ and throughput, the periodicity of the trend and the correlatedness can be exploited to reduce the number of required samples.

In LTE, physical layer indicators RSRP, RSRQ, RSSI (received signal strength indicator), and SINR (signal to interference and noise ratio) are measured based on cell-specific reference signals. In 5G, the same KPIs are defined for secondary synchronization signals and channel state information reference signals [2] and are measured for individual beams.

In 5G new radio, in frequency range 1 (410 MHz – 7125 MHz) [24], for static beams, we expect similar behavior with RSRP being stable for longer periods and other KPIs (RSRQ, SINR, throughput) being subject to time-of-day activities of users in the serving beam and neighboring beams.

References

[1] V. Raida *et al.* (2020) LTE DL static rural and urban outdoor dataset. [Online]. Available: http://doi.org/10.23728/b2share.f5df0b362b7e473c825776ec166e658f

[2] 3GPP, "Physical layer; Measurements," TS 36.214, 2020, v. 15.5.0.

[3] Android Developers. (2020) CellSignalStrengthLte. [Online]. Available: https://developer.android.com/reference/android/telephony/CellSignalStrengthLte

[4] Rundfunk und Telekom Regulierungs-GmbH. (2020) RTR – NetTest. [Online]. Available: https://www.netztest.at/en/

[5] V. Raida, P. Svoboda, and M. Rupp, "Real world performance of LTE downlink in a static dense urban scenario – an open dataset," in *2020 IEEE GLOBECOM*, Dec. 2020. [Online]. Available: https://owncloud.nt.tuwien.ac.at/index.php/s/rMbPJLRgRRqHiaW

[6] S. Kumar *et al.*, "LTE radio analytics made easy and accessible," in *Proceedings of the 2014 ACM Conference on SIGCOMM*, 2014.

[7] J. Cainey, B. Gill, S. Johnston, J. Robinson, and S. Westwood, "Modelling download throughput of LTE networks," in *39th Annual IEEE Conference on Local Computer Networks Workshops*, 2014.

[8] J. Sommers and P. Barford, "Cell vs. WiFi: On the performance of metro area mobile connections," in *Proceedings of the 2012 Internet Measurement Conference*. Association for Computing Machinery, 2012.

[9] R. K. Polaganga and Q. Liang, "Self-similarity and modeling of LTE/LTE-A data traffic," *Measurement*, vol. 75, pp. 218 – 229, 2015.

[10] A. Bokani, M. Hassan, S. S. Kanhere, J. Yao, and G. Zhong, "Comprehensive mobile bandwidth traces from vehicular networks," in *Proceedings of the 7th International Conference on Multimedia Systems*. Association for Computing Machinery, 2016.

[11] J. van der Hooft, S. Petrangeli, T. Wauters, R. Huysegems, P. R. Alface, T. Bostoen, and F. De Turck, "HTTP/2-based adaptive streaming of HEVC video over 4G/LTE networks," *IEEE Communications Letters*, vol. 20, no. 11, pp. 2177–2180, 2016.

[12] V. Raida, P. Svoboda, and M. Rupp, "Modified dynamic time warping with a reference path for alignment of repeated drive-tests," in *2020 IEEE 92nd Veh. Technol. Conf.*, Oct. 2020, submitted for review.

[13] B. Meixner, J. W. Kleinrouweler, and P. Cesar, "4G/LTE channel quality reference signal trace data set," in *Proceedings of the 9th ACM Multimedia Systems Conference*, 2018.

[14] D. Raca, J. J. Quinlan, A. H. Zahran, and C. J. Sreenan, "Beyond throughput: A 4G LTE dataset with channel and context metrics," in *Proceedings of the 9th ACM Multimedia Systems Conference*, 2018.

[15] V. Raida, P. Svoboda, and M. Rupp. (2020) LTE DL static urban indoor dataset. [Online]. Available: http://doi.org/10.23728/b2share.2367746915e34d1ca4bda84193f8056b

[16] Keysight Technologies. (2020) Nemo Handy handheld measurement solution. [Online]. Available: https://www.keysight.com/en/pd-2767485-pn-NTH00000A/nemo-handy

[17] V. Raida, M. Lerch, P. Svoboda, and M. Rupp, "Deriving cell load from RSRQ measurements," in *2018 Network Traffic Measurement and Analysis Conference (TMA)*, 2018.

[18] J. Dugan *et al.* (2020) iPerf – The TCP, UDP and SCTP network bandwidth measurement tool. [Online]. Available: https://iperf.fr/

[19] LG Electronics. (2020) LG K4 LTE Smartphone | LG Österreich. [Online]. Available: https://www.lg.com/at/handys/lg-K120E-k4-lte

[20] 3GPP, "User equipment (UE) radio access capabilities," TS 36.306, 2020, v. 15.8.0.

[21] Android Developers. (2020) CellIdentityLte. [Online]. Available: https://developer.android.com/reference/android/telephony/CellIdentityLte

[22] LTE-Anbieter. (2014) Huawei LTE Cube E5180. [Online]. Available: https://www.lte-anbieter.info/lte-hardware/all/huawei-lte-cube-e5180

[23] R. P. Foundation. (2020) Raspberry Pi 3 Model B. [Online]. Available: https://www.raspberrypi.org/products/raspberry-pi-3-model-b/

[24] 3GPP, "NR; User Equipment (UE) radio transmission and reception; Part 1: Range 1 Standalone," TS 38.101-1, 2020, v. 16.3.0.